Variations in the magnetic anisotropy properties of epitaxial CrO_2 films as a function of thickness

Guoxing Miao and Gang Xiao
Physics Department, Brown University, Providence, Rhode Island 02912, USA

Arunava Gupta
MINT Center, Department of Chemistry, Chemical and Biological Engineering, University of Alabama, Tuscaloosa, Alabama 35487, USA

(Received 8 June 2004; revised manuscript received 5 October 2004; published 23 March 2005)

The strain resulting from lattice mismatch has a strong influence on the magnetic anisotropy of epitaxial CrO_2 films grown on (100) TiO_2 substrates by chemical vapor deposition. Thus the magnetic easy axis at room temperature changes orientation with thickness, switching from the in-plane *c*-axis ([001]) direction for films thicker than 250 nm to the *b*-axis ([010]) direction for thinner films ($<$50 nm). Similarly, over a thickness range, a change of the easy axis direction is observed with lowering temperature. The easy-axis switching characteristics can be understood by a simple model that invokes the competing influence of magnetocrystalline and strain anisotropies with varying degree of strain relaxation. Interestingly, films of intermediate thicknesses (50–250 nm) exhibit double-switching phenomena, corresponding to the easy axis being oriented both along the *b* and *c*-axis directions. This unusual switching behavior is considered to result from an inhomogeneous distribution of strain in the films, where a portion of the film remains highly strained while the balance is partially relaxed. With increasing thickness, the switching attributed to the latter increases in magnitude while that from the heavily strained component steadily decreases until it is no longer observable for films thicker than 250 nm.

DOI: 10.1103/PhysRevB.71.094418 PACS number(s): 75.30.Gw, 75.70.−i, 76.60.Es, 75.50.Ss

I. INTRODUCTION

The unique properties of chromium dioxide (CrO_2) have attracted much interest in recent years.[1–6] Band structure calculations have predicted the material to be completely spin polarized, with the minority spin band possessing a gap at the Fermi level whereas the Fermi level intersects the band for the majority electron spin.[7–9] Such a distinctive band characteristic—termed half-metallic—has now been experimentally confirmed.[10,11] Superconducting point-contact measurements, using Andreev reflection spectroscopy, have provided spin polarization (P) values for CrO_2 as high as 98.4% at low temperatures, among the largest for all ferromagnetic materials.[10] The high value of P makes CrO_2 an ideal system for the study of the physical properties of half-metallic systems. Moreover, it is an attractive material for spintronic devices such as magnetic tunnel junctions and spin valves.[12–15] For the practical implementation of CrO_2-based devices, it is important to gain a better understanding of its switching characteristics and magnetic anisotropy, and explore possible approaches to control these properties. The current work attempts to provide a comprehensive investigation of the magnetic properties of epitaxial CrO_2 thin films, with an emphasis on the strong sensitivity of its magnetic anisotropy to the film thickness and temperature. We have found that variations in the film thickness have a significant influence on its magnetic switching characteristics. In particular, the magnetic easy axis can be reoriented with changing thickness. Moreover, for a fixed film thickness, varying the temperature can also effectively change the switching field, or even rotate the easy direction. We attribute the diverse anisotropic properties of the epitaxial CrO_2 films to the inherent stain and its evolution as a function of thickness and temperature.

II. EXPERIMENT

CrO_2 has a tetragonal rutile structure ($a=b=4.421$ Å, $c=2.916$ Å) that is reasonably well lattice matched with rutile TiO_2 ($a=b=4.594$ Å, $c=2.958$ Å), which we use as a substrate material for our studies. We have deposited epitaxial CrO_2 thin films in a chemical vapor deposition (CVD) reactor consisting of a quartz tube placed inside a two-zone furnace with independent temperature control of the two zones.[16,17] Before film growth, the single crystal (100) TiO_2 substrates are cleaned with organic solvents and dilute hydrofluoric (HF) acid solution and loaded into the CVD chamber. The films are grown at a substrate temperature of 400 °C in the primary zone, with the solid CrO_3 precursor placed in the secondary sublimation zone of the furnace that is heated to about 260 °C. Oxygen is used as the carrier gas with a constant flow rate of 100 sccm. We have measured the magnetic properties of the deposited films at room temperature using a vibrating sample magnetometer (VSM), (DMS model 10), as well as a Quantum Design superconducting quantum interference device (SQUID) magnetometer for low temperature measurements. In addition, the films have been structurally characterized using a Philips X'pert high-resolution x-ray diffraction system.

III. RESULTS AND DISCUSSION

The epitaxial (100) CrO_2 films that we have deposited display a Curie temperature (T_C) of ~390 K independent of

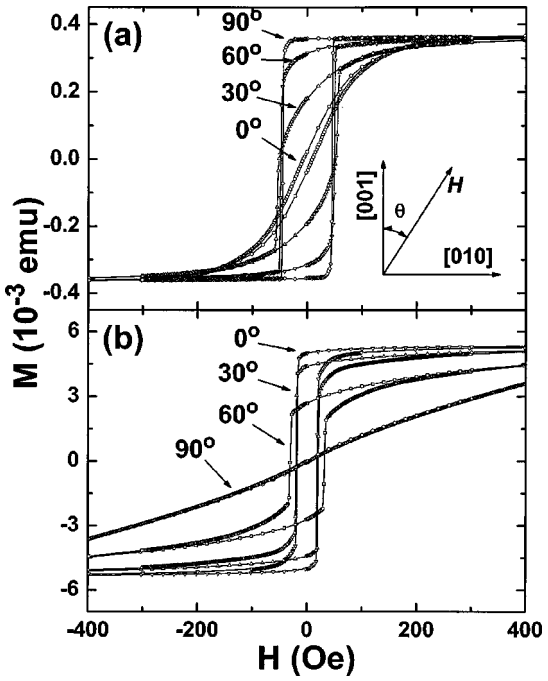

FIG. 1. Hysteresis loops at various measurement angles for (a) 30 nm CrO_2 and (b) 430 nm CrO_2 film at 300 K.

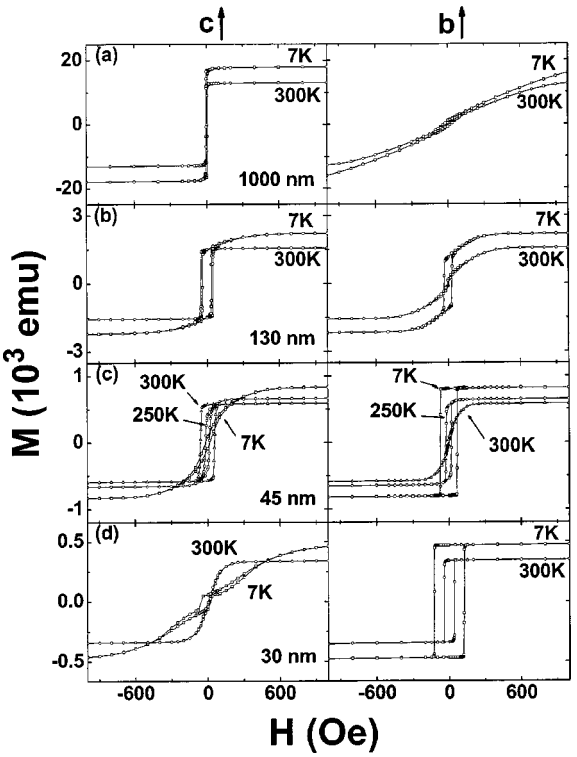

FIG. 2. Hysteresis loops of CrO_2 films of various thicknesses. (a) 1000 nm film with bulk-like switching characteristics; (b) 130 nm film with partial easy axis rotation; (c) 45 nm film exhibiting easy axis rotation with temperature; around; and (d) 30 nm film with complete easy axis rotation.

the film thickness. The room temperature and 7 K saturation magnetization M_s has been determined to be 475 and 640 emu/cm^3, the corresponding anisotropy energy constant K_1 are 2.2×10^5 and 4.5×10^5 erg/cm^3, and K_2 are 4×10^4 and 3×10^4 erg/cm^3, respectively.[18] All the magnetic measurements reported in this paper have been carried out on blanket films of dimension 5×5 mm^2, with the film thickness being no more than 2×10^{-4} of the lateral dimension. We thus expect the magnetization to be confined to the plane of the substrate with negligible demagnetizing field ($H_D<0.5$ Oe) and shape anisotropy in-plane. The thinnest film we have studied is about 9 nm thick (corresponding to about 40 atomic layers) and the surface anisotropy contribution, as usually observed in ultrathin (1–10 atomic layers) transition metal films, is not expected to be significant. Thus, there are two competing anisotropies present in the as-deposited CrO_2 films—the magnetocrystalline and the strain anisotropy that are considered significant. The former, a volume effect, is an intrinsic property of the material that favors the magnetic easy axis to orient along the in-plane *c* direction, as observed both for bulk samples[18] and also for thick films.[17,19] The latter is an interface effect, and strained thin films grown on (100) TiO_2 substrates exhibit magnetic easy-axis alignment along the *b* direction, since the lattice misfit is larger along the *b* than in the *c* direction (3.91% vs 1.44%).[17] We have found that the relative magnitude of these two anisotropies is dependent on the film thickness. Based on simple estimates, one expects the ratio of the magnetocrystalline energy to the strain anisotropy energy to be approximately proportional to the film thickness *t*, which is related to the volume-to-surface ratio. We show, based on a model of residual strain in the film, that a somewhat more complex thickness dependence is appropriate, as described later in this paper.

A. Variations in the switching characteristics with film thickness and temperature

Figure 1 shows the angular dependence of the hysteresis loops for a thick (~430 nm) and a thin (~30 nm) CrO_2 film at room temperature. The magnetic axis changes from the *c* direction in the thick film to the *b* direction in the thin film. As has been previously shown,[19] the hysteresis loops of epitaxial (100) CrO_2 films can be reasonably described by coherent rotation of $\boldsymbol{M}$ followed by Kondorskii-type domain wall motion,[27,28] where the magnetic reversal occurs when the projection of the applied field on the magnetic easy direction reaches a critical value, i.e., $H_s(\psi)\cos\psi=H_s(0)$, where ψ is the angle between the applied field and the easy axis.

We have found that the temperature also strongly affects the anisotropy in CrO_2 films. Figure 2 shows the magnetic hysteresis loops, measured along the *c* and *b*-axis directions at $T=7$ and 300 K, for films of four different thicknesses. It is interesting to note that: (a) for the bulklike 1000 nm film, the *c* axis is the magnetic easy axis at both temperatures; (b) for the intermediate 130 nm film, at room temperature, the *c* axis is the easy axis, but there exist contribution from another in-plane perpendicular component as will be discussed later; (c) for the 45 nm film, the easy *c* axis at room temperature becomes the hard axis at low temperature; and (d) for the thinnest (30 nm) film, the easy axis is the *b* axis at both temperatures.

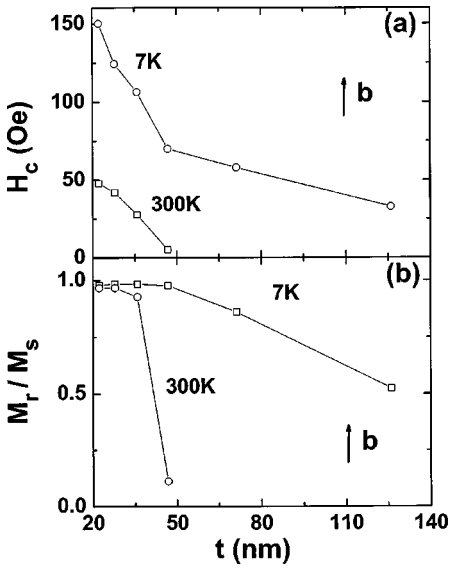

FIG. 3. Thickness dependence of (a) the coercive field (H_c) and (b) the magnetic remanence (M_r/M_s) of CrO_2 films measured at 300 and 7 K, respectively, along the *b*-axis direction.

Figure 3 summarizes two key magnetic hysteresis parameters as a function of the film thickness—the coercive field (H_c) and the remanance (M_r/M_s), defined as the ratio between the remanant magnetization at zero field and the saturation magnetization, measured with the external field aligned along the *b*-axis direction. When the thickness is below 35 nm, the *b* axis is clearly the magnetic easy axis at temperatures between 7 and 300 K, as evidenced by the nearly 100% value of M_r/M_s. The value of H_c is observed to decrease with increasing thickness. Near the critical thickness of about 50 nm at 300 K, both M_r/M_s and H_c vanish, indicating that the easy axis has switched to the *c* direction at this thickness. However, at $T=7$ K, the critical thickness for complete easy axis rotation is much higher, indicating a much stronger influence of the strain in the film at low temperatures.

Figure 4 summarizes the effect of temperature on easy axis rotation for various thicknesses. Here the remanance is plotted as a function of the measurement temperature. The temperature induced easy axis rotation is best seen for the 45 nm film. As the temperature is lowered below 300 K, the easy axis gradually changes from the *c*-axis to the *b*-axis direction for this film. The strain variation with temperature is largely a result of the differences in the thermal expansion coefficient between the film and the substrate and their anisotropies in the two crystallographic directions.

B. Influence of the total strain anisotropy on switching

Next, we attempt to explain the thickness dependence of the magnetic anisotropy and easy axis rotation. We describe the free energy of the system as

$$E = K_0 - K_1 \cos^2\theta - K_2 \cos^4\theta + (K_{\sigma c}\sin^2\theta + K_{\sigma b}\cos^2\theta)$$
$$= \text{const} - K_1 \cos^2\theta + K_\sigma \cos^2\theta - K_2 \cos^4\theta \quad (1)$$

where K_1 and K_2 are the magnetocrystalline anisotropy energy constants; $K_{\sigma b}$ and $K_{\sigma c}$ are the strain anisotropy energy constants associated with the *b* and *c*-axis directions, respectively; $K_\sigma = K_{\sigma b} - K_{\sigma c} = \frac{3}{2}\lambda(\sigma_b - \sigma_c) = \frac{3}{2}\lambda Y(\varepsilon_b - \varepsilon_c)$; θ is the angle between the magnetization and the *c* axis; σ_b and σ_c are stresses.[20] We have represented K_σ in terms of the strain components in the two directions by using the relationship $K_\sigma = \frac{3}{2}\lambda Y\varepsilon$, where λ is the magnetostriction coefficient, Y is the Young's modulus, and ε is the strain.[20]

It is well known that for epitaxial growth on lattice-mismatched substrates the film usually grows coherently strained to match the substrate for thin layers. However, above a critical thickness, dislocations are generated to relieve the misfit strain. By minimizing the sum of the energy of the misfit dislocations and the elastic misfit strain, Matthews and Blakeslee (M-B)[21–23] have derived the thickness dependence for the residual equilibrium strain

$$\varepsilon = \frac{1 - \nu\cos^2\varphi}{8\pi(1+\nu)\cos\phi}\frac{b}{t}\ln\left(\frac{4t}{b}\right), \quad (2)$$

where *b* is the magnitude of the Burgers vector of the dislocation, and $\alpha = \{(1-\nu\cos^2\varphi)/[8\pi(1+\nu)\cos\phi]\}$ is a constant that depends on the Poisson ratio ($\nu \cong 0.3$), the angles of the Burgers vector with respect to the dislocation line (φ), and the angles between the interface and the normal to the slip

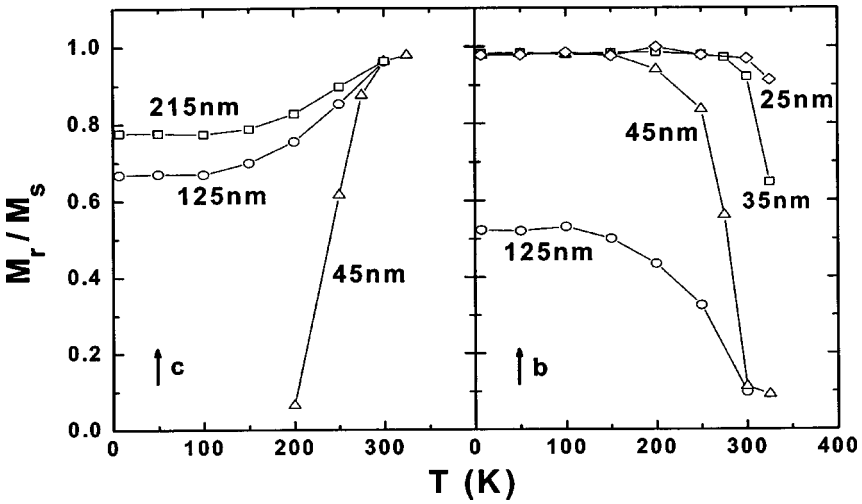

FIG. 4. Temperature dependence of the magnetic remanence (M_r/M_s) measured along the *c* and *b*-axis directions for different thickness CrO_2 films.

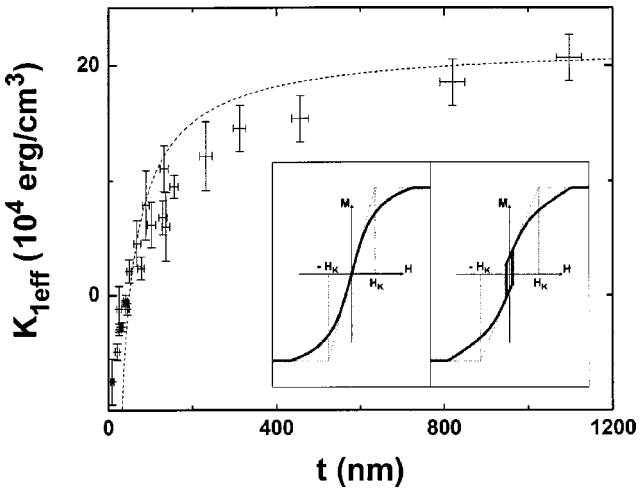

FIG. 5. Thickness dependence of the effective anisotropy constant $K_{1\,\mathrm{eff}}$, The dashed line is generated using Eq. (3), as described in the text. Inset illustrates the procedure for determining the anisotropy field from the hard axis hysteresis loops of films exhibiting either regular or double switching characteristics.

plane (ϕ). By neglecting the K_2 term in Eq. (1), we can relate the effective magnetic anisotropy energy constant $K_{1\,eff}=K_1-K_\sigma$ to the film thickness t:

$$K_{1\,\mathrm{eff}} = K_1 - \frac{3}{2}\lambda \mathrm{Y}\alpha\left[\frac{b}{t}\ln\left(\frac{4t}{b}\right) - \frac{c}{t}\ln\left(\frac{4t}{c}\right)\right]. \qquad (3)$$

In the above equation we have approximated the magnitudes of the Burgers vectors in the b and c directions with the corresponding lattice parameters. From Eq. (3) it is seen that the ratio between K_1 and K_σ is proportional to $[t/(\ln t+\mathrm{const})]$ for films thicker than a few tens of nanometers (i.e., when $t \gg b,c$).

By analyzing the anisotropy fields based on the hysteresis loop measured along the hard axis direction at room temperature (e.g., Fig. 1), we have determined the values of $K_{1\,eff}$ for CrO_2 films over a large range of thicknesses, as shown in Fig. 5. The dashed line is generated using Eq. (3), indicating that the thickness dependence of anisotropy can be reasonably well predicted by the theory. For generating the plot a value of $K_1=2.2\times10^5$ erg/cm^3 at room temperature has been assumed based on experimental measurements of CrO_2 bulk single crystals,[18] and we also used the fact that $\sim$50 nm is the thickness around which the easy axis reversal occurs (Fig. 3). We have carried out x-ray measurements of the off-axis (220) and (202) peaks of CrO_2 to determine the in-plane b and c lattice parameters, and the value of α is determined to be 0.39 from the experimentally measured strain in a 50 nm CrO_2 film. If we assume the Young's modulus to be 2.5×10^{12} dyn/cm^2, as in the case of bulk TiO_2, the magnetostriction coefficient of CrO_2 is estimated to be 9.4×10^{-6}. It should be noted that the value of α is larger than what is normally expected from M-B model. This is because the simple M-B model does not take into account the force due to the tension at the surface steps and the stacking faults, both having the effect of increasing the predicted residual strain.[23] The lattice parameters of films at various

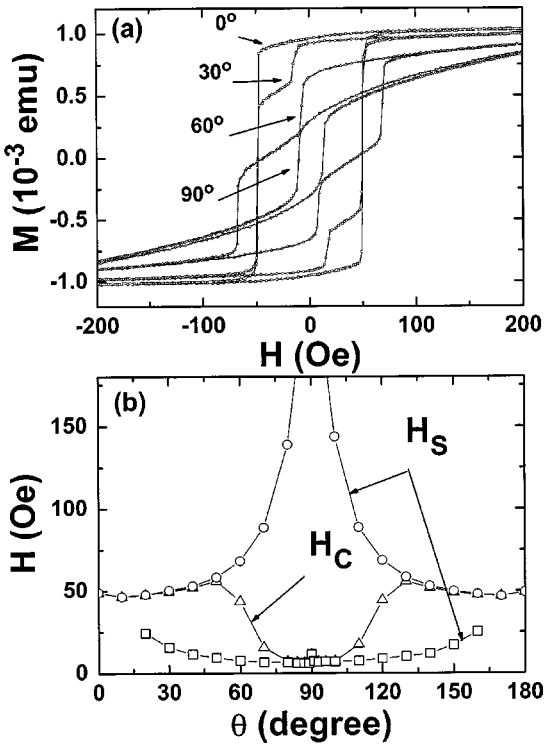

FIG. 6. (a) Hysteresis loops of a 90 nm CrO_2 film as a function of measurement angle from the c-axis direction, exhibiting double switching behavior. (b) Angular dependence of the two switching fields (H_s) and the coercive field (H_c) for the 90 nm film.

thickness also show that the actual decrease of strain as a function of thickness is slower than that predicted by Eq. (2), as is also reflected in comparing the theoretical curve and the actual data points in Fig. 5. If we use a simple power law to characterize such a decrease, the dependence is closer to $t^{-0.3}$ rather than $\{[\ln(t/b)]/t\}\approx t^{-1}$. A slower relaxation rate than predicted by the equilibrium M-B model is commonly observed for epitaxial oxide films, and has been attributed to kinetic barriers in the propagation and multiplication of the misfit dislocations needed for the relaxation due to the ionic nature of the oxides.[24,25]

From the above discussion, it is clear that the nature of the strain relaxation as a function of thickness has a strong influence on the magnetic anisotropy of CrO_2 films. The crystalline and strain anisotropy directions for growth on (100) TiO_2 substrate are orthogonal to each other. If coherent rotation can be achieved for all thickness, the easy axis should be along the c direction for films over 50 nm, and along the b direction for films below 50 nm, as suggested by the change in the sign of $K_{1\,eff}$ in Fig. 5. However, our results show that the anisotropy of CrO_2 films is more complicated than a simple switching of easy axis for an intermediate range of thicknesses.

C. Influence of inhomogeneous strain on the switching characteristics: Double switching in intermediate thickness films

In the thickness range of about 50–250 nm, we find that the CrO_2 films do not exhibit a simple uniaxial switching

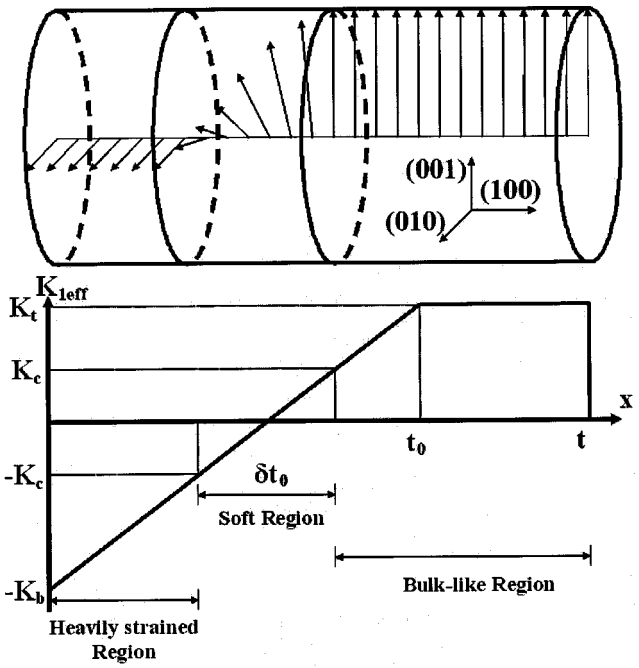

FIG. 7. Schematic drawing of an "intermediate" thickness CrO_2 film illustrating the spin directions and the effective anisotropy constant as a function of distance from the substrate interface.

behavior. Figure 6(a) shows the hysteresis loops for a 90 nm film with fields applied along various angles relative to the *c* axis. Clearly, there exist two different switching fields. The angular dependence of the two switching fields H_s are shown separately in Fig. 6(b). H_s is defined as the field where the magnetization switching occurs, and is determined from the maximum in the slope of the hysteresis curve. The coercive field H_c, where the magnetization changes sign, is also plotted in Fig. 6(b). It is clear that the two distinct switching fields are 90° out of phase, corresponding to the easy axis being along the *b* or *c* direction. A similar behavior is observed for thicker films up to about 250 nm, with the *c*-axis switching component increasing in magnitude while the *b*-axis component decaying with increasing thickness.

The original M-B model was developed for thin films in which the thickness is not much larger than the spacing between neighboring edge dislocation lines, and therefore the strain distribution is assumed to be homogeneous throughout the film. In reality, especially for thick oxide films, the strain is more concentrated near the interface and is gradually relaxed by forming dislocations. This is evidenced from the nonuniform distribution of dislocations at various depths in the films.[25,26] For simplicity, we have constructed a model by neglecting higher order contributions from strain and assuming that the film strain varies linearly from the substrate interface up to a thickness t_0, and that there is no strain present above this thickness. As a result, K_2 is a constant and $K_{1\,eff}$ varies linearly up to t_0 and then remains constant after reaching the bulk value (Fig. 7), i.e.:

$$K_{1\,eff} = \begin{cases} -K_b + \dfrac{K_t + K_b}{t_0} x, & (x < t_0) \\ K_t, & (x > t_0) \end{cases}, \tag{4}$$

here K_b and K_t are the effective anisotropy constant at the film-substrate interface and the top surface, respectively. This simple model captures the essential characteristics that the strain is more concentrated near the interface, and $K_{1\,eff}$ averaged over the whole film retains the $1/t$ dependence predicted by the M-B model. At a certain depth into the film, the strain anisotropy and crystalline anisotropy balance each other and results in near-zero effective anisotropy in its vicinity. The region with $|K_{1\,eff}| < K_c$ is considered a soft layer with a width δt_0 and is sandwiched between the top and the bottom "hard(er)" layers (Fig. 7). The anisotropy of the top layer, which is dominated by the crystalline anisotropy, has an easy direction along the *c* axis. While the bottom layer, dominated by epitaxial strain, has an easy direction along the *b* axis. The intermediate soft layer will assume a spin configuration as that in a 90° Bloch domain wall. Such a system can be considered in analogy with a spring magnet system.[29,30] Although the hysteresis loops of these films look very similar to those reported for spring magnets with a hard-magnetic/soft-magnetic bilayer,[29,30] we have experimentally found that neither of the switching fields in these samples is reversible. This is not unexpected since both surfaces of the soft layer are clamped between two rigid magnetic layers with mutually perpendicular orientations.

The total energy of such a system can be denoted by

$$E = A\int_0^t \left(\frac{d\theta}{dx}\right)^2 dx - \int_0^t [K_{1\,eff}(x)\cos^2\theta(x) + K_2\cos^4\theta(x)]dx - \int_0^t HM_s\cos\theta(x)dx, \tag{5}$$

here A is the exchange stiffness constant, N is the total number of atomic layers in the soft region and is proportional to δ, d is the spacing between two atomic layers, and $\theta(x)$ is the spin polarity with respect to the *c* axis at position *x*. The first term is the exchange energy coming primarily from the soft region, the second term is the anisotropy energy including contributions from both the strain and crystalline anisotropies, and the third term is the Zeeman energy. The minimization of the energy term in Eq. (5) with respect to $\theta(x)$ is nontrivial, so we make the assumption that the spins vary linearly with *x* within the soft region, and by minimizing the total energy with respect to the domain wall thickness δ, the ground state energy of this approximated spin configuration can be obtained. It needs to be pointed out that for very thin films, the domain wall region can expand over t_0 (i.e., $K_c > K_t$), and we have also taken such spin configurations into consideration. Then we compare the calculated minimum energy to the energy when all spins are aligned along a single direction $\{E = -\cos^2\phi\int_0^t [K_{1\,eff}(x) + K_2]dx$, *when* $\theta(x) \equiv \phi\}$ in order to determine whether this spring magnet-type configuration indeed has a lower energy than the completely spin parallel configuration. For obtaining a reasonable estimate, we use the following values:

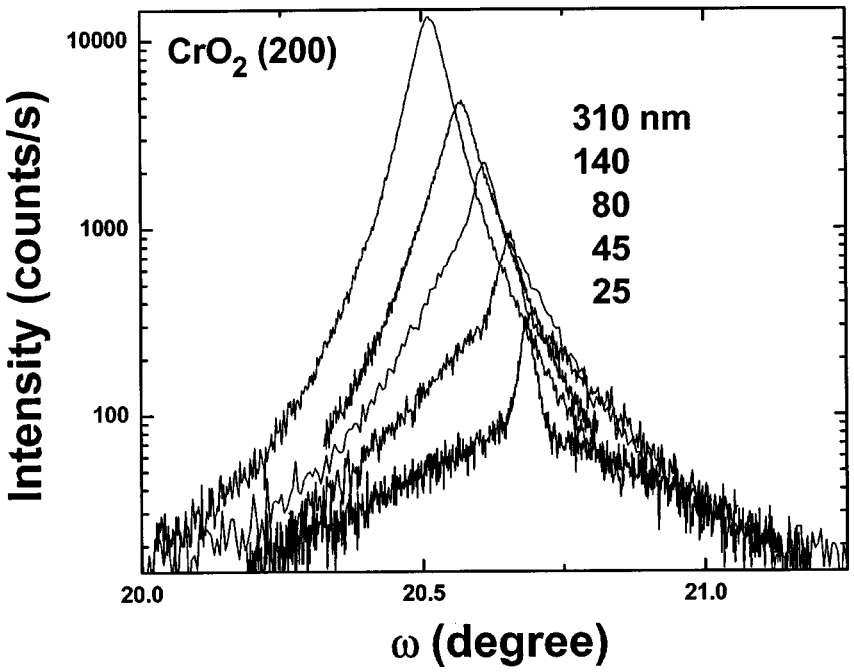

FIG. 8. X-ray rocking curves of the (200) CrO_2 peak for films of different thicknesses as marked in the figure.

$$A \approx 4.6 \times 10^{-7} \text{ erg/cm},$$

$$K_t \approx K_{bulk} \approx 2.2 \times 10^5 \text{ erg/cm}^3,$$

$$K_b \approx \tfrac{3}{2}\lambda Y(3.91\,\% - 1.44\,\%) \approx 8.4 \times 10^5 \text{ erg/cm}^3.$$

A is estimated based on the Curie temperature of CrO_2, K_t is taken as the bulk anisotropy constant of CrO_2 by assuming that the top part of the film is fully relaxed, and K_b is estimated by assuming that the film at the bottom interface is fully strained and by using the estimated magnetostriction coefficient described earlier in this paper.

It should be emphasized that t_0 is the extended region of the strain starting from the interface and is actually determined during the film growth process, therefore it should be dependent on the film thickness. Nevertheless, we can reasonably explain our results by assuming that $t_0 = 40$ nm in all measured films. Under this assumption, a critical film thickness of 55 nm can be determined. For films below 55 nm, since a spring magnet formation is not energetically favorable and the spin parallel configuration along the b axis is the ground state, the easy axis of the film is completely aligned along the b axis. For intermediate thickness films (e.g., Fig. 6), a spring magnet spin configuration is produced, with a bottom layer of ~9 nm, a soft layer of ~46 nm, and the remaining thickness for the top layer. The hysteresis loops should contain two separate switching fields in this case, and each set of switching fields roughly obey a Kondorskii-type domain wall motion,[27,28] as observed in our samples. Despite the success in predicting the double switching behavior, the remnance from the actually measured hysteresis loops does not exactly match the calculated values (around 75% for magnetic fields along the c-direction, and 45% along the b-direction). This suggests that the soft layer domain wall position in the film is probably also dependent on field angle. Knowledge of the actual strain distribution will be needed to explain the details of the observed hysteresis loops. For very thick films [e.g., Fig. 1(b)], the contribution from the bottom strained layer is very weak compared to the top layer, and can no longer be clearly separated. In fact, the assumption that all the strain is concentrated in the 55 nm range near the interface is not really valid for very thick films, and a broader distribution of strain results in smearing the hysteresis loops.

Our model suggests that the large strain and its inhomogeneous distribution through the film are key to the understanding the magnetic double switching behavior. It is worth asking the question as to what would happen if the strain is not sufficiently strong. For an order of magnitude estimate, the following criteria can be used for films with broad strain distributions to estimate whether or not the double switching is justified in a given system, $\frac{1}{2}K_b t_0 \geqslant \frac{\beta}{2}\pi[A(K_b+K_t)]^{1/2}$, here β is a dimensionless factor depending on the distribution of strains, in our case, it is 0.22. In other words, double magnetic switching will occur when the energy decrease caused by rotating the bottom layer to its easy direction is larger than the energy increase resulting from the formation of a 90° domain wall. Consequently, one can see that no double switching would be observable when the strain is low, or when the material is magnetically hard and have high exchange stiffness.

Evidence for inhomogeneous distribution of strain in the films with two components has been obtained from x-ray measurements as a function of thickness. Figure 8 shows the ω-rocking curve measurements of the CrO_2 (200) peak for different thickness films. The thinnest film (25 nm), that is expected to be heavily strained, exhibits a sharp peak with a full width at half maximum (FWHM) of 0.034°. A broader component develops with increasing thickness until it completely dominates; resulting in a FWHM of 0.064° for the 310 nm. The two components are clearly noticeable for the intermediate thickness films for which double switching is observed. This strongly suggests that there are two distinct

layers in these films, with a thin heavily strained layer near the substrate interface region and a thicker partially relaxed layer that has increased mosaicness due to random formation of dislocations. For very thin films, the energy cost to form a domain wall is so large that uniaxial switching is retained even though there still exist two distinct layers. The separation into layers having different strain has also been reported for epitaxial growth of perovskite films, such as $SrRuO_3$ and $La_{0.6}Sr_{0.4}MnO_3$ on (100) $SrTiO_3$ substrate.[25,26] High-resolution transmission electron microscopy (TEM) studies will be needed to gain better understanding of the strain distribution in CrO_2 films.

IV. SUMMARY AND CONCLUSIONS

In summary, we have studied the in-plane magnetic properties of epitaxial CrO_2 films deposited on (100) TiO_2 substrates. Complete easy axis rotation and double switching phenomena have been observed as a function of film thickness and temperature. We attribute the switching characteristics to the strain induced by the lattice mismatch with the substrate. Unlike the thickness dependence, it is presently not possible to explain the details of the temperature-dependent anisotropy behavior of the films. This is because of the lack of experimental data on the temperature and anisotropy dependence of the thermal expansion and the magnetostriction coefficients and the Young's modulus of both the film and the substrates. Experimental results have shown that the crystalline anisotropy (characterized by K_1) in bulk single crystal increases monotonically from room temperature to low temperatures.[18] The observation of easy axis rotation with decreasing temperature suggests that the strain anisotropy must be increasing at a faster rate at low temperatures for it to dominate the switching characteristics. The increased strain could possibly be caused by the differences in the thermal expansion coefficients between the CrO_2 film and the TiO_2 substrate, and its anisotropy in the two directions.

ACKNOWLEDGMENTS

We thank W. D. Doyle for a critical review of the manuscript and providing valuable suggestions. This work was supported by the National Science Foundation Grant Nos. DMR-0306711 and DMR-0080031.

[1] H. Y. Hwang and S. W. Cheong, Science **278**, 1607 (1997).
[2] J. M. D. Coey, A. E. Berkowitz, L. Balcells, F. F. Putris, and A. Barry, Phys. Rev. Lett. **80**, 3815 (1998).
[3] A. Gupta and J. Z. Sun, J. Magn. Magn. Mater. **200**, 24 (1999).
[4] K. Suzuki and P. M. Tedrow, Appl. Phys. Lett. **74**, 428 (1999).
[5] J. Dai and J. Tang, J. Appl. Phys. **89**, 6763 (2001).
[6] A. Sokolov, C.-S. Yang, L. Yuan, S.-H. Liou, R. Cheng, H.-K. Jeong, T. Komesu, B. Xu, C. N. Borca, P. A. Dowben, and B. Doudin, Europhys. Lett. **58**, 448 (2002).
[7] K. Schwarz, J. Phys. F: Met. Phys. **16**, L211 (1986).
[8] S. P. Lewis, P. B. Allen, and T. Sasaki, Phys. Rev. B **55**, 10 253 (1996).
[9] M. A. Korotin, V. I. Anisimov, D. I. Khomskii, and G. A. Sawatzky, Phys. Rev. Lett. **80**, 4305 (1998).
[10] Y. Ji, G. J. Strijkers, F. Y. Yang, C. L. Chien, J. M. Byers, A. Anguelouch, G. Xiao, and A. Gupta, Phys. Rev. Lett. **86**, 5585 (2001); A. Anguelouch, A. Gupta, G. Xiao, D. W. Abraham, Y. Ji, S. Ingvarsson, and C. L. Chien, Phys. Rev. B **64**, 180408(R) (2001).
[11] J. S. Parker, S. M. Watts, P. G. Ivanov, and P. Xiong, Phys. Rev. Lett. **88**, 196601 (2002).
[12] A. M. Bratkovsky, Appl. Phys. Lett. **72**, 2334 (1998).
[13] A. Gupta, X. W. Li, and G. Xiao, J. Appl. Phys. **87**, 6073 (2000).
[14] S. M. Watts, S. Wirth, S. vonMolnar, A. Barry, and J. M. D. Coey, Phys. Rev. B **61**, 9621 (2000).
[15] A. Gupta, X. W. Li, and G. Xiao, Appl. Phys. Lett. **78**, 1894 (2001).
[16] S. Ishibashi, T. Namikawa, and M. Satou, Jpn. J. Appl. Phys. **17**, 249 (1978).
[17] X. W. Li, A. Gupta, and G. Xiao, Appl. Phys. Lett. **75**, 713 (1999).
[18] D. S. Rodbell, J. Phys. Soc. Jpn. **21**, 1224 (1966).
[19] F. Y. Yang, C. L. Chien, E. F. Ferrari, X. W. Li, G. Xiao, and A. Gupta, Appl. Phys. Lett. **77**, 286 (2000).
[20] B. D. Cullity, *Introduction to Magnetic Materials* (Addison-Wesley, London, 1972).
[21] J. W. Matthews and A. E. Blakeslee, J. Cryst. Growth **27**, 118 (1974).
[22] J. W. Matthews, J. Vac. Sci. Technol. **12**, 126 (1975).
[23] *Epitaxial Growth*, edited by J. W. Matthews (Academic Press, New York, 1975).
[24] T. Suzuki, Y. Nishi, and M. Fujimoto, Philos. Mag. A **79**, 2461 (1999).
[25] S. H. Oh and C. G. Park, J. Appl. Phys. **95**, 4691 (2004).
[26] Y. Konishi, M. Kasai, M. Izuma, M. Kawasaki, and Y. Tokura, Mater. Sci. Eng., B **56**, 158 (1998).
[27] E. I. Kondorskii, J. Phys. (USSR) **2**, 161 (1940).
[28] W. D. Doyle, J. E. Rudisill, and S. Shtrikman, J. Phys. Soc. Jpn. **17**, 567 (1962).
[29] E. E. Fullerton, J. S. Jiang, M. Grimsditch, C. H. Sowers, and S. D. Bader, Phys. Rev. B **58**, 12 193 (1998).
[30] E. E. Fullerton, J. S. Jiang, and S. D. Bader, J. Magn. Magn. Mater. **200**, 392 (1999).